# Supplemental figures and tables

**Figure S1. Schematic representation of GP130 and IL-6 family cytokine signaling.**

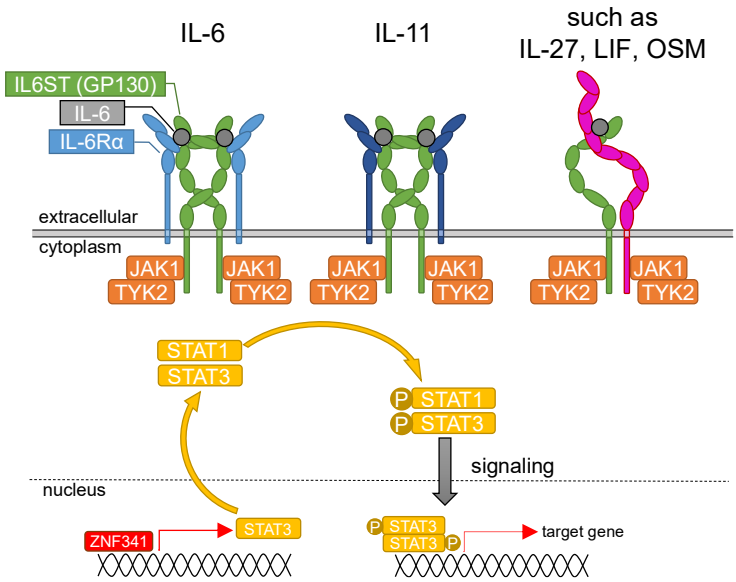


IL-6, the IL-6 receptor, and GP130 form a hexamer at the cell surface, with two molecules each. The same is true for IL-11, while IL-27, LIF, and OSM form a trimer with one molecule each. This leads to signaling to the nucleus through phosphorylation of Jaks and STATs, resulting in the expression of a variety of genes. STAT3 expression is regulated by ZNF341.

**Figure S2. The p.H855P mutation is an allele identical to p.K702fs.**

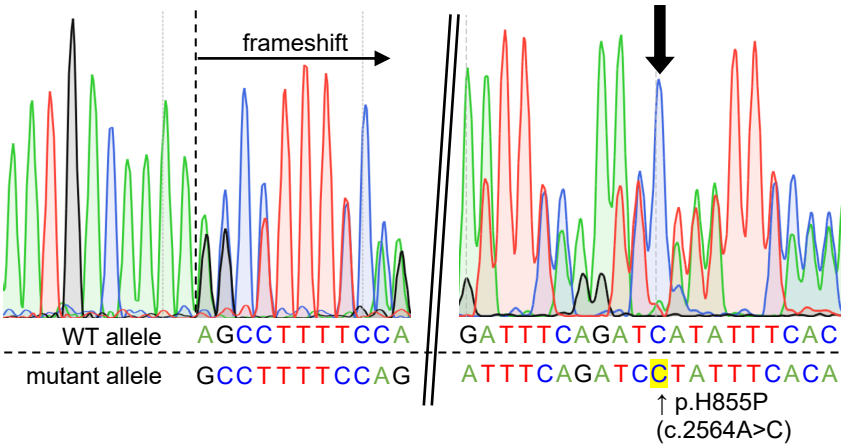


The waveform pattern of the Sanger sequence indicated that p.H855P and p.K702fs are located on the same allele. If they were on different alleles, the waveforms (black arrows) would be in the A and C heteropattern.

**Figure S3. Deep immunophenotyping of patients with AD-*IL6ST* mutation Y759Wfs.**

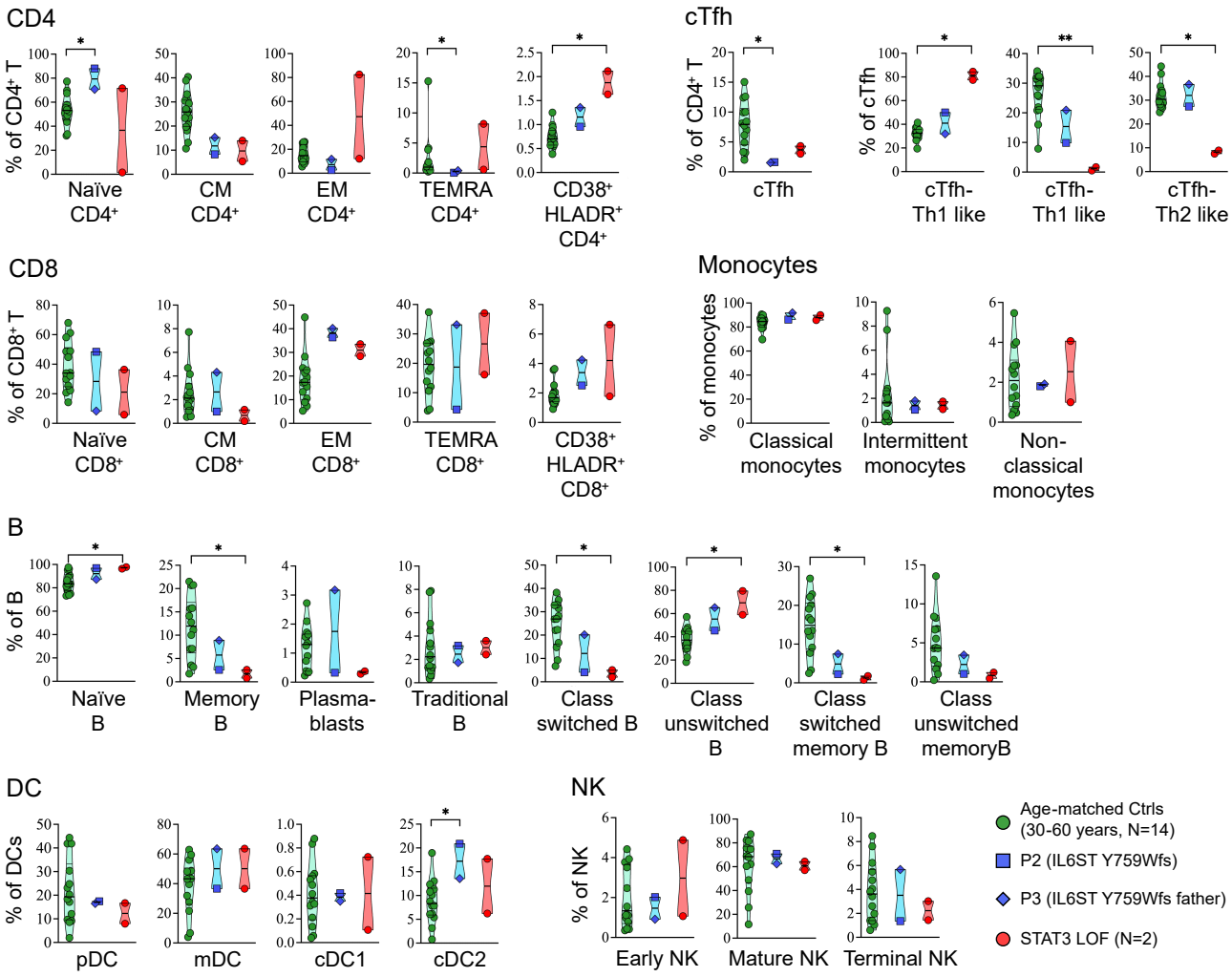


This deep immunophenotyping for patient PBMCs was performed using Aurora (Cytek). Age-matched healthy controls (30-60 years, N=14) are represented by green dots, P2 by blue squares, P3 by blue diamonds, and the patients with heterozygous DN *STAT3* mutation patients (p.V637M, p.Y657C) by red dots (N=2). Statistical analysis was done with two-tailed Mann–Whitney U test. *; P<0.05, **; P<0.01. CM, central memory; EM, effector memory; TEMRA, terminally differentiated effector memory T cells re-expressing CD45RA; cTfh, circulating follicular helper T; pDC/mDC/cDC, plasmacytoid/monocyte-derived/conventional dendritic cell.

**Figure S4. Determination of the amount of WT plasmid to be used in the experiments.**

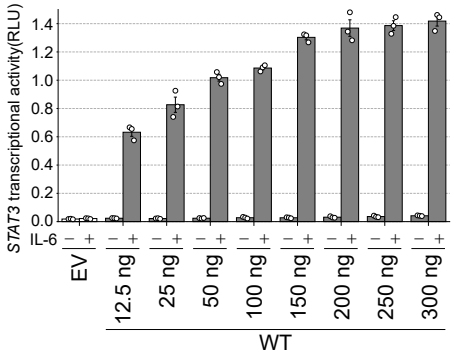


STAT3 transcriptional activity of GP130-KO-HEK293T cells transfected with several amounts of WT, and EV was added to adjust the total amount of DNA transfected into the cells. Bars and error bars are the means and SEM of technical triplicates. This experiment was independently performed three times, and a representative result is shown. EV, empty vector; mut, mutant.

**Figure S5. The hetero 2 variants (K702fs, Y759Wfs) are less active than haploinsufficiency due to the DN effect.**

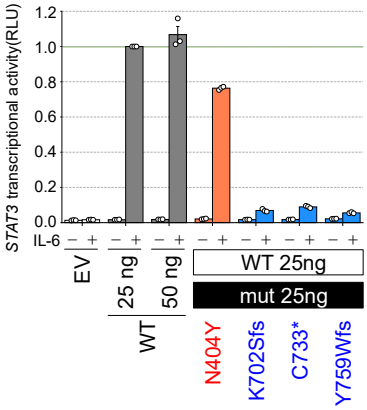


STAT3 transcriptional activity of GP130-KO-HEK293T cells transfected with either WT (25 ng or 50 ng) or WT and variants at a 1:1 ratio (WT:mut = 25 ng:25 ng) and stimulated with or without IL-6. RLU values were normalized to the post-stimulation WT (25 ng) values as 1. Bars and error bars are the means and SEM of technical triplicates. This experiment was independently performed three times, and a representative result is shown. EV, empty vector; mut, mutant.

**Figure S6. Patient PBMCs show cell surface GP130 accumulation and impaired STAT3 phosphorylation.**

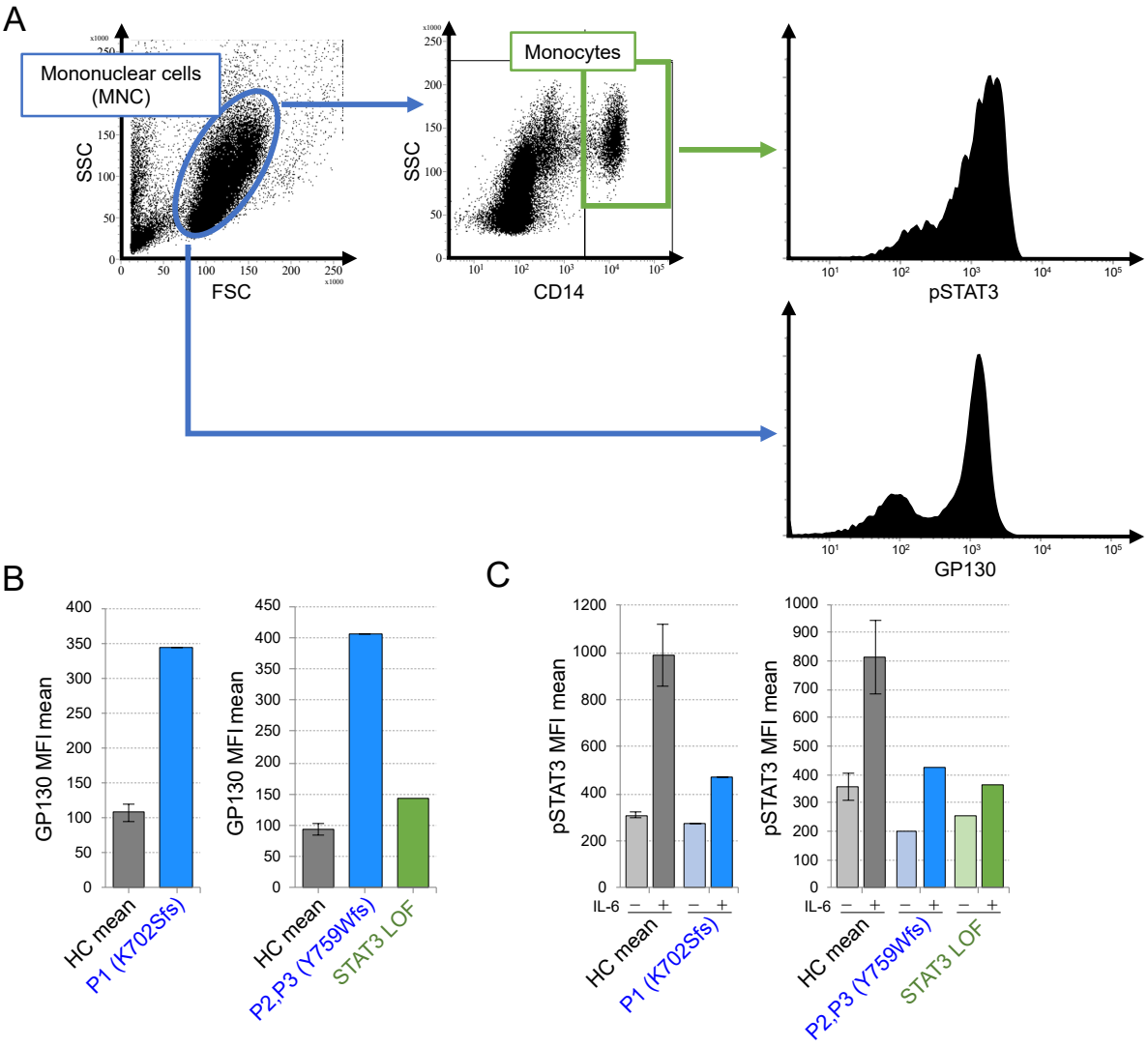


**(A)** Gating scheme of PBMCs. Mononuclear cells were gated based on forward and side scatter profiles (left panel). The MFI of GP130 was evaluated in mononuclear cells (bottom right panel). CD14-positive cells were gated within the mononuclear cells (monocytes, middle panel) and the MFI of pSTAT3 was evaluated (top right panel). **(B)** Quantitative MFI values for cell surface GP130 in PBMCs from patients and healthy subjects are shown; for HCs, values are the average of 3 samples, for *IL6ST* (Y759Wfs) patients, values are the average of P2 and P3. Each experiment was independently performed twice and a representative result is shown. **(C)** PBMCs from patients and healthy subjects were cultured and stimulated with IL-6 (50 ng/mL) or left unstimulated. The quantitative MFI values of pSTAT3 gated with CD14 after fixation and permeabilization of the collected cells are shown; for HCs, the values are the average of 3 samples, for *IL6ST* (Y759Wfs) patients, values are the average of P2 and P3. Each experiment was independently performed twice and a representative result is shown. HC; healthy control, MFI; mean fluorescence intensity, LOF; loss-of-function.

**Figure S7. The mutants, which are predicted to be AD, are less active than the AR mutant and exhibit a DN effect.**

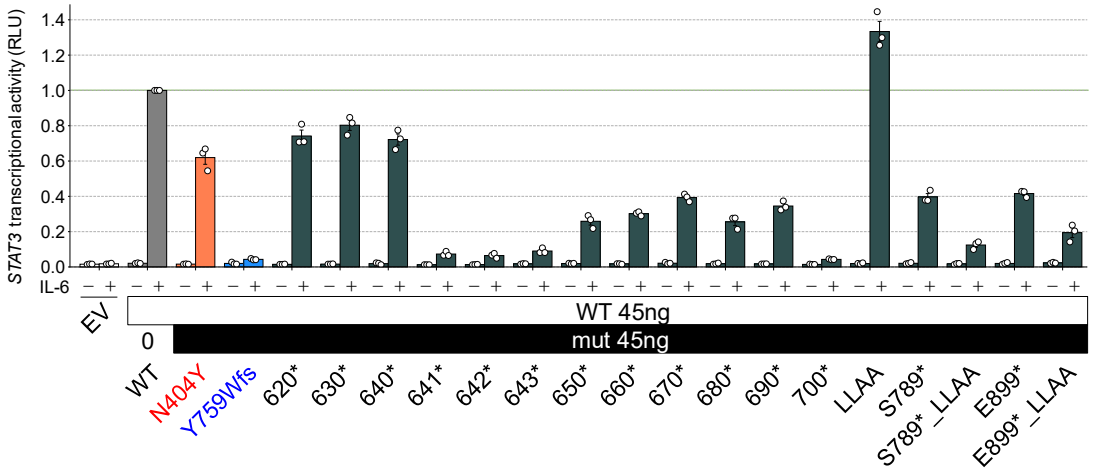


STAT3 transcriptional activity of GP130-KO-HEK293T cells transfected with either 45 ng of WT alone or with WT or its variants at a 1:1 ratio (WT:mut = 45 ng:45 ng) and stimulated with or without IL-6. RLU values were normalized to the poststimulation WT values as 1. Bars and error bars are the means and SEM of technical triplicates. This experiment was independently performed three times, and a representative result is shown. EV, empty vector; mut, mutant.

**Figure S8. Functional analysis of nonsense or frameshift variants listed in gnomAD.**

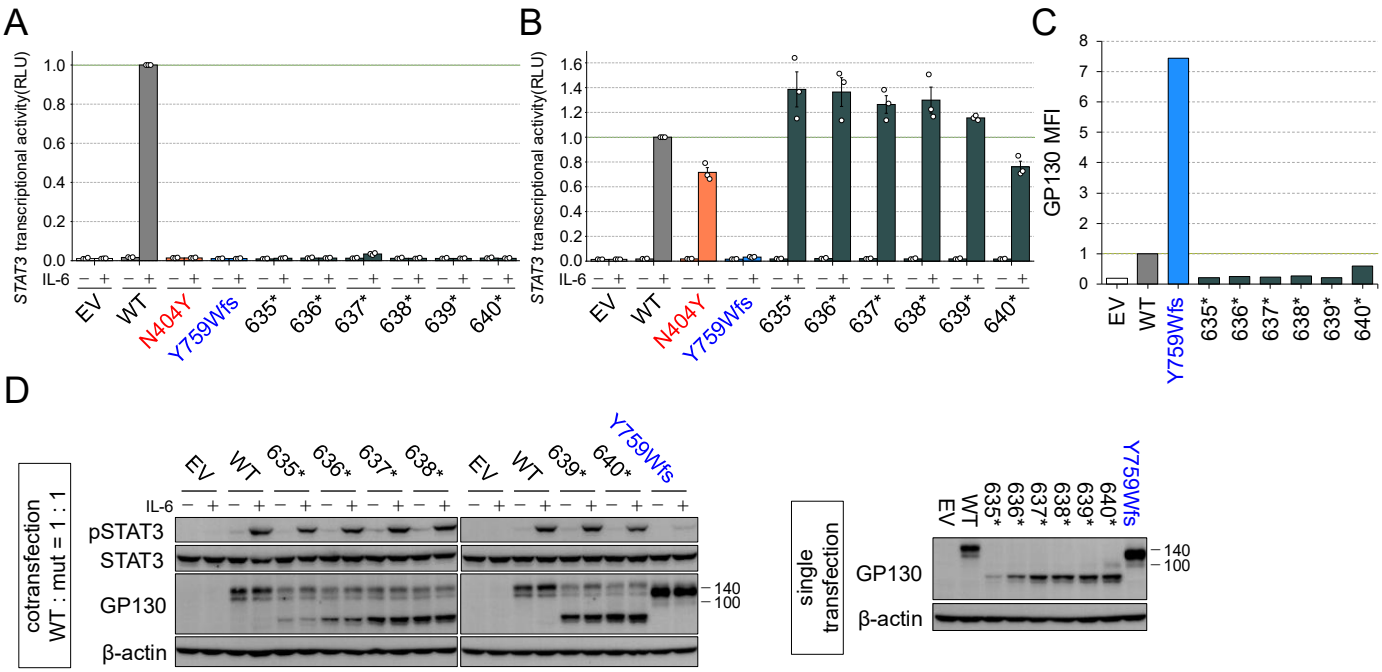


**(A,B)** STAT3 transcriptional activity in GP130-KO-HEK293T cells transfected with WT and/or variants and stimulated with or without IL-6 (**A**: single, **B**: 1:1 ratio). RLU values were normalized to the poststimulation WT value of 1. Bars and error bars are the means and SEM of technical triplicates. This experiment was independently performed three times, and a representative result is shown.

**(C)** MFI of cell surface GP130 expression in transfected GP130-KO-HEK293T cells. MFI values were normalized to the WT values as 1. This experiment was independently performed three times, and a representative result is shown. **(D)** Immunoblotting of pSTAT3, STAT3 and GP130 in GP130-KO-HEK293T cells transfected with WT and/or variants and stimulated with or without IL-6 (above: cotransfection at a 1:1 ratio, below: single). β-Actin was used as a loading control. This experiment was independently performed twice, and a representative result is shown. EV, empty vector; mut, mutant.

**Figure S9. Functional analysis of nonsense or frameshift variants listed in gnomAD.**

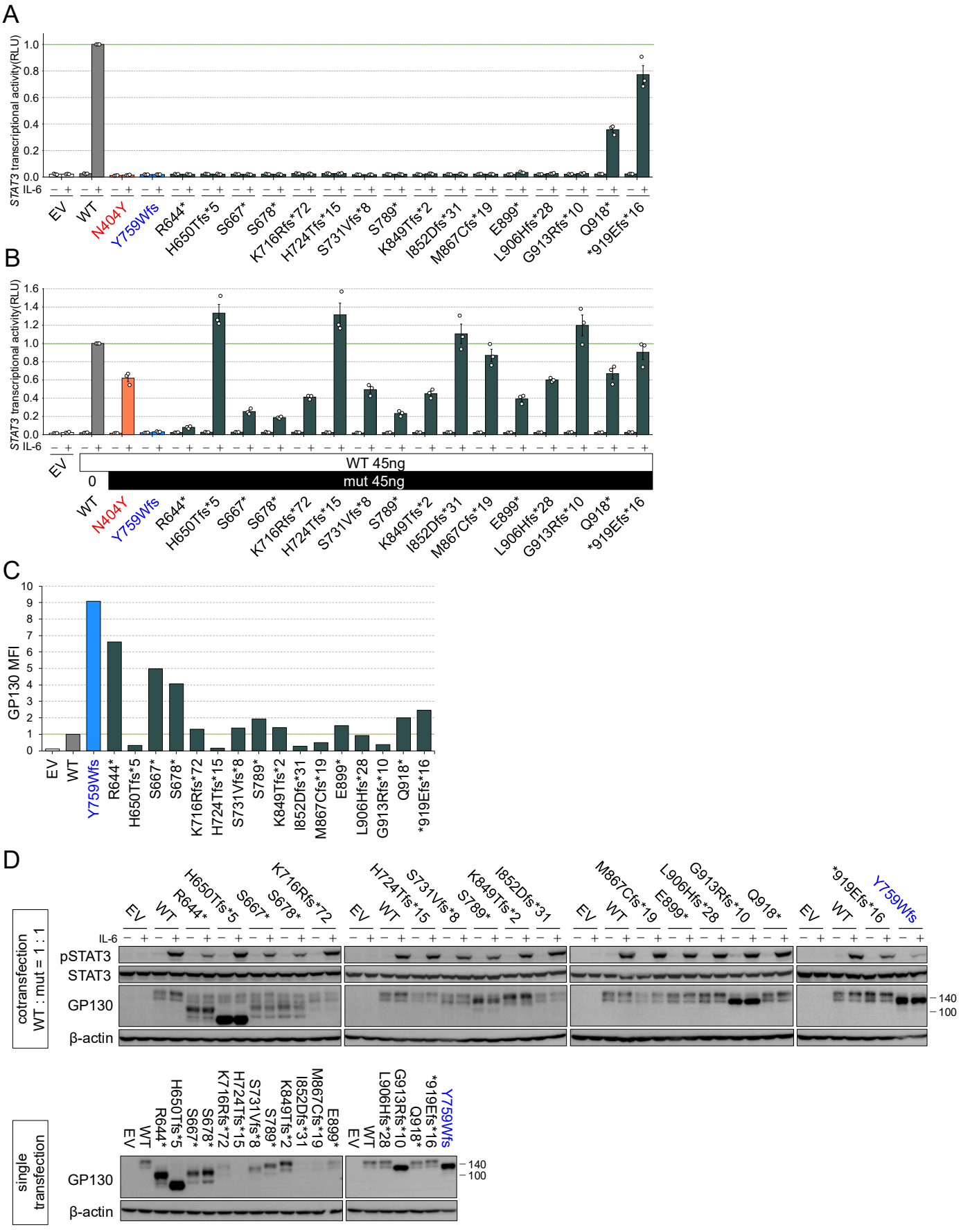

**(A,B)** STAT3 transcriptional activity in GP130-KO-HEK293T cells transfected with WT and/or variants and stimulated with or without IL-6 (**A**: single, **B**: 1:1 ratio). RLU values were normalized to the poststimulation WT value of 1. Bars and error bars are the means and SEM of technical triplicates. This experiment was independently performed three times, and a representative result is shown.
**(C)** MFI of cell surface GP130 expression in transfected GP130-KO-HEK293T cells. MFI values were normalized to the WT values as 1. This experiment was independently performed three times, and a representative result is shown. **(D)** Immunoblotting of pSTAT3, STAT3 and GP130 in GP130-KO-HEK293T cells transfected with WT and/or variants and stimulated with or without IL-6 (above: cotransfection at a 1:1 ratio, below: single). β-Actin was used as a loading control. This experiment was independently performed twice, and a representative result is shown. EV, empty vector; mut, mutant.

**Table S1. Deep immunophenotyping of patients with the AD-*IL6ST* mutation K702Sfs.**

| Patient | Family 1 P1 | | Reference Value (20) |
|---|---|---|---|
| Variant allele | K702Sfs*7 H855P | | |
| B cells (% of lymphocytes) | 0.4 | low | 12.2±4.4 |
| Memory B cells (% of CD19+) | 12 | low | 18.5±8.2 |
| T cells (% of lymphocytes) | 83.1 | high | 67.8±5.4 |
| CD4+ T cells (% of CD3+) | 60.1 | normal | 59.9±9.9 |
| Naïve T cells (% of CD3+CD4+) | 85.7 | high | 47.2±9.3 |
| Memory T cells (% of CD3+CD4+) | 11.9 | low | - |
| Th1 cells (% of CD3+CD4+CD45RO+) | 4.94 | low | 22.6±8.7 |
| Th2 cells (% of CD3+CD4+CD45RO+) | 71.9 | high | 35.3±13.8 |
| Th17 cells (% of CD3+CD4+CD45RO+) | 21.4 | normal | 23.7±4.3 |
| CD8+ T cells (% of CD3+)[%] | 38.4 | normal | 34.1±8.7 |
| CD8+ Naïve T cells (% of CD3+CD8+) | 96.6 | high | 64.2±7.1 |
| CD8+ Memory T cells (% of CD3+CD8+) | 2.5 | low | - |

**Table S2. The nonsense or frameshift variants within the intracellular domain registered in gnomAD and the UK Biobank.**

| variants | | Allele Frequency | | Reference |
|---|---|---|---|---|
| amino acid | codon | gnomAD | UK Biobank | |
| p.Arg644Ter | c.1930C>T | 7.13E-07 | 4.26E-06 | |
| p.His650ThrfsTer5 | c.1947dup | 6.91E-07 | N.D | |
| p.Ser667Ter | c.2000C>A | 6.89E-07 | N.D | |
| p.Ser678Ter | c.2033C>A | 1.20E-06 | 1.06E-06 | |
| p.Lys716ArgfsTer72 | c.2147del | 1.59E-06 | N.D | |
| p.His724ThrfsTer15 | c.2168dup | 6.84E-07 | N.D | |
| p.Ser731ValfsTer8 | c.2190dup | 6.58E-06 | N.D | Arlabosse et al. (16) |
| p.Ser789Ter | c.2366C>G | 6.84E-07 | N.D | |
| p.Lys849ThrfsTer2 | c.2542_2545dup | 6.84E-07 | N.D | |
| p.Ile852AspfsTer31 | c.2552dup | 6.84E-07 | N.D | |
| p.Met867CysfsTer19 | c.2599del | 1.20E-06 | 1.06E-06 | |
| p.Glu899Ter | c.2694dup | 6.57E-06 | N.D | |
| p.Leu906HisfsTer28 | c.2716_2719del | 6.84E-07 | N.D | |
| p.Gly913ArgfsTer10 | c.2736dup | 1.59E-06 | N.D | |
| p.Gln918Ter | c.2752C>T | 2.40E-06 | 4.26E-06 | |
| p.Ter919GlufsTer16 | c.2755del | 1.20E-06 | N.D | |

N.D, no data.

**Table S3. The antibodies used in the panel of deep immunophenotyping.**

| Color | marker | Vender | Catalog | Clone |
|---|---|---|---|---|
| BUV395 | CD45RA | BD Biosciences | 740315 | 5H9 |
| Ghost Dye UV450 | Live/dead | Tonbo Biosciences | 13-0868-T500 | |
| BUV496 | CD16 | BD Biosciences | 612944 | 3G8 |
| BUV563 | CCR5 | BD Biosciences | 741401 | 2D7/CCR5 |
| BUV615 | CD314(NKG2D) | BD Biosciences | 751232 | 1D11 |
| BUV661 | CD39 | BD Biosciences | 749967 | TU66 |
| BUV737 | CD56 | BD Biosciences | 612766 | NCAM16.2 |
| BUV805 | CD8 | BD Biosciences | 612889 | SK1 |
| BV421 | CCR7 | BioLegend | 353208 | G043H7 |
| SuperBright436 | CD123 | Thermo Fisher Scientific | 62-1239-42 | 6H6 |
| eFluor 450 | CD11c | Thermo Fisher Scientific | 48-0116-42 | 3.9 |
| BV510 | CD3 | BioLegend | 344828 | SK7 |
| cFluor V547 | CD20 | Cytek Biosciences | R7-20111 | 2H7 |
| BV570 | IgM | BioLegend | 314518 | MHM-88 |
| BV605 | CCR4 | BioLegend | 359418 | L291H4 |
| BV650 | CD28 | BioLegend | 302946 | CD28.2 |
| BV711 | CCR6 | BioLegend | 353436 | G034E3 |
| BV750 | CXCR5 | BD Biosciences | 747111 | RF8B2 |
| BV785 | PD-1 | BioLegend | 329930 | EH12.2H7 |
| cFluor B515 | cD141 | Cytek Biosciences | R7-20113 | M80 |
| cFluor B532 | CD57 | Cytek Biosciences | RC-00127 | HNK-1 |
| cFluor B548 | CD14 | Cytek Biosciences | R7-20115 | 63D3 |
| PerCP | CD45 | Tonbo Biosciences | 67-9459-T500 | 2D1 |
| PerCP-Cy5.5 | CD2 | BioLegend | 309226 | TS1/8 |
| PerCP-Vio700 | TCRgd | Miltenyi Biotec | 130-113-506 | 11F2 |
| cFluor BYG750 | IgD | Cytek Biosciences | RC-00521 | IgD26 |
| PE | NKG2C(CD159C) | Miltenyi Biotec | 130119776 | REA205 |
| cFluor YG584 | CD4 | Cytek Biosciences | R7-20041 | SK3 |
| PE-Dazzle594 | CD337(NKp30)(NCR3) | BioLegend | 325232 | p30-15 |
| cFluor YG610 | CD24 | Cytek Biosciences | R7-20659 | SN3 |
| PE-Cy5 | FAS | BioLegend | 305610 | DX2 |
| PE-Fire 700 | CD25 | BioLegend | 356146 | M-A251 |
| PE-Cy7 | CXCR3 | BioLegend | 353720 | G025H7 |
| PE-Fire810 | HLA-DR | BioLegend | 307683 | L243 |
| APC | NKG2A | Miltenyi Biotec | 130113563 | REA110 |
| cFluor R668 | CD1c | Cytek Biosciences | R7-20119 | L161 |
| Spark NIR685 | CD19 | BioLegend | 302270 | HIB19 |
| cFluor R720 | CD127 | Cytek Biosciences | RC-00009 | A019D5 |
| APC H7 | CD27 | BD Biosciences | 560222 | M-T271 |
| APC-Fire 810 | CD38 | BioLegend | 356644 | HIT2 |